

Rates of Jets Produced in Association with W and Z Bosons

K.S. Grogg on behalf of the CMS Collaboration
 Department of Physics, University of Wisconsin, Madison, WI, USA

Presented here is a study of jets produced in association with vector bosons production in pp collisions at $\sqrt{s} = 7$ TeV using the full CMS 2010 data set, corresponding to an integrated luminosity of $36 \pm 1.4 \text{ pb}^{-1}$. The transverse energy distribution of the reconstructed leading jets is measured and compared to theoretical expectations. The jet multiplicity distributions are corrected for efficiency and unfolded. The ratios of multiplicities, $\sigma(V + \geq n \text{ jets})/\sigma(V + \geq (n-1) \text{ jets})$ and $\sigma(V + \geq n \text{ jets})/\sigma(V)$ where n stands for number of jets, are also presented along with the first test of the Berends-Giele scaling at $\sqrt{s} = 7$ TeV.

1. Introduction

The production of hadronic jets in association with W and Z vector bosons (denoted $V + \text{jets}$) provides the means for a rigorous study of perturbative QCD. Because the production of vector bosons with jets constitutes a significant source of background in searches for new physics and for studies of the top quark, a precise measurement of the $V + n$ jets cross section and an understanding of the kinematics is essential.

This proceedings presents results obtained with the 2010 data sample of the CMS experiment at the Large Hadron Collider (LHC) at CERN, based on $36.1 \pm 1.4 \text{ pb}^{-1}$ of integrated luminosity collected in proton-proton collisions at $\sqrt{s} = 7$ TeV. To reduce theoretical and systematic uncertainties, we measure the $V + n$ jets cross sections relative to the inclusive W and Z cross sections. We also measure the cross section ratios $\sigma(V + \geq n \text{ jets})/\sigma(V + \geq (n-1) \text{ jets})$ from which we are able to test Berends-Giele scaling [1]. The complete $V + \text{jets}$ analysis is reported in [2].

2. Samples and Reconstruction

Monte Carlo (MC) simulation samples are used both for comparison to data and to unfold the jet multiplicity distributions. Simulated events with a W or a Z boson are generated with the MADGRAPH [3] event generator, producing parton-level events with a vector boson and up to four jets on the basis of a matrix-element calculation. MADGRAPH is interfaced to the PYTHIA [4] program for parton shower simulation. Top pair ($t\bar{t}$) and single top processes are generated with MADGRAPH also. Multijet and $\gamma + \text{jets}$ processes are generated with PYTHIA alone. For comparison to the data distributions, the simulation samples are normalized to NNLO or NLO cross sections and scaled to the luminosity. The PYTHIA parameters for the underlying event are set to the “Z2” tune, a modification of the “Z1” tune described in [5]. Comparisons are also made to the “D6T” tune [6]. Minimum-bias events are superimposed on the simulated events to represent “pile-up” found in data from multiple proton interactions in a single bunch crossing.

Muons are reconstructed using both the silicon tracker and muon chambers. Identification based on compatibility sub-detector measurements is used to assure quality muons with p_T resolution of about 1-2%. Electron candidates are produced by matching tracks to superclusters constructed from EM calorimeter (ECAL) energy deposits with an E_T resolution of about 1%.

A particle flow (PF) algorithm is used to reconstruct both the missing transverse energy (\cancel{E}_T) and the jets in the event. The PF algorithm creates a complete event description by collecting information from all of the sub-detectors and linking it together. Objects are initially formed into the categories of muons, electrons, photons, charged hadrons, and neutral hadrons. From these elements the jets and missing transverse energy, \cancel{E}_T , are reconstructed.

The \cancel{E}_T is reconstructed as the opposite of the sum of the transverse momentum of all of the PF particles. Jets are reconstructed from PF objects by means of the anti- k_T algorithm [7] with a size parameter of $R = 0.5$. Jet energy corrections (JEC) are applied to account for the jet energy response as a function of η and p_T and corrections are made to the jet energy for the effect of pile-up.

3. Signal Selection

Signal selection begins with the identification of a “leading lepton”, either an electron or a muon. The bulk of the lepton selection follows the standard established by the measurement of the inclusive W and Z cross sections [8].

arXiv:1110.0213v1 [hep-ex] 2 Oct 2011

For electron candidates we require $p_T > 20$ GeV and that the ECAL cluster lies in the fiducial region of $|\eta| < 2.5$ while excluding the region $1.4442 < |\eta| < 1.566$ in order to reject electrons close to the barrel/endcap transition where cables and services reduce detectability. A series of quality requirements including identification, isolation, and conversion rejection are then applied to the electron. For the leading electron, the values of the different quality requirements are chosen such that they correspond to an electron efficiency of about 80% as evaluated with a MADGRAPH + PYTHIA simulated sample.

If there is a second electron of $p_T > 10$ GeV and it is within the ECAL fiducial volume, passes a looser set of quality cuts (corresponding at an efficiency of about 95%), and forms an invariant mass with the leading electron between 60 GeV and 120 GeV, then the event is placed in the Z + jets sample. Otherwise, the event is assigned to the W + jets sample. Events with a muon with $p_T > 15$ GeV and $|\eta| < 2.4$ are then rejected from the W + jets sample to reduce $t\bar{t}$ contamination.

The muon selection starts by requiring the presence of an isolated muon in the region $|\eta| < 2.1$ with $p_T > 20$ GeV passing the requirements described in [8] along with a transverse impact parameter $|d_{xy}| < 2$ mm to suppress cosmic-ray muon background. A requirement that the combined activity of the tracker and calorimeters around the muon is less than 0.15 relative to the muon p_T results in quality muons and background suppression. If there is (is not) a second muon of $p_T > 10$ GeV accepted in the range $|\eta| < 2.5$ such that the dimuon invariant mass lies within the region 60 GeV to 120 GeV, then the event is assigned to the Z + jets (W + jets) sample.

For both W + jets samples, the transverse mass, M_T , is constructed from the lepton and \cancel{E}_T , $M_T = \sqrt{2p_T \cancel{E}_T(1 - \cos \Delta\phi)}$ where $\Delta\phi$ is the angle in the xy -plane. To avoid a region at low M_T containing essentially no signal we require that $M_T > 20$ GeV.

4. Jet Rates

Jets must first satisfy identification criteria to eliminate jets originating from noise in the calorimeter. We require that the jets fall within the tracker acceptance of $|\eta| < 2.4$. The observed transverse momentum distributions for the leading jet are shown in Figs. 1 and 2. The data is in good agreement with the MADGRAPH predictions normalized to the NNLO cross sections. For the W sample, we have required $M_T > 50$ GeV in order to reduce backgrounds.

Events are assigned to exclusive bins of jet multiplicity by counting the number of jets in the event with $p_T > 30$ GeV. The observed distributions of the exclusive numbers of reconstructed jets in the W and Z samples are shown in Figs. 3 and 4, respectively. The distributions from simulation are also shown, with overall good agreement.

One of the most important backgrounds in the W sample comes from $t\bar{t}$ events. These events contain two b -quark jets. Jets are b -tagged with a tagging algorithm that requires at least two tracks in the jet with a significance on the transverse impact parameter greater than 3.3. This choice of cut results in a b -tagging efficiency of about 62% and a mis-tagging rate of about 2.9% [9]. The number of b -tagged jets, $n_{b\text{-jet}}$, is used in the fitting method to separate W from top events.

5. Acceptance and Efficiency

In order to avoid model-dependent results, we quote all results within the lepton and jet acceptance, and only correct for efficiency of the selection. The efficiencies for lepton reconstruction, identification, isolation and trigger are obtained by a tag-and-probe method performed on $Z/\gamma^* + \text{jets}$ data. The tag-and-probe sample for the measurement of a given efficiency contains events selected with two lepton candidates of invariant mass in the range [60-120] GeV. One lepton candidate, called the ‘‘tag’’, satisfies all selection requirements. The other lepton candidate, called the ‘‘probe’’, is selected with criteria that depend on which efficiency is being examined. The signal yields are obtained both for events in which the probe lepton passes or in which it fails the selection criteria considered.

Fits are performed to the invariant-mass distributions of the pass and fail subsamples to extract the Z signal events. The measured efficiency is calculated from the relative level of signal in the pass and fail subsamples. The lepton selection efficiency is the product of the reconstruction efficiency, the identification and isolation efficiency, and the trigger efficiency. Each of these efficiencies is calculated as a function of the jet multiplicity in the event. The ratio of tag-and-probe results for the $Z/\gamma^* + \text{jets}$ data sample are combined with the full efficiency estimated from the W+jets and Z+jets selection in simulation.

For electrons we find that the efficiencies are roughly 70% (60%) for the W + jets ($Z/\gamma^* + \text{jets}$) signal events with variations of a few percent across different jet multiplicity bins.

For muons, the efficiencies are measured as a function of p_T and η in the highest statistics bins ($n = 0$ and $n = 1$). Due to the isolation requirement, the efficiencies also exhibit a significant dependence on the observed

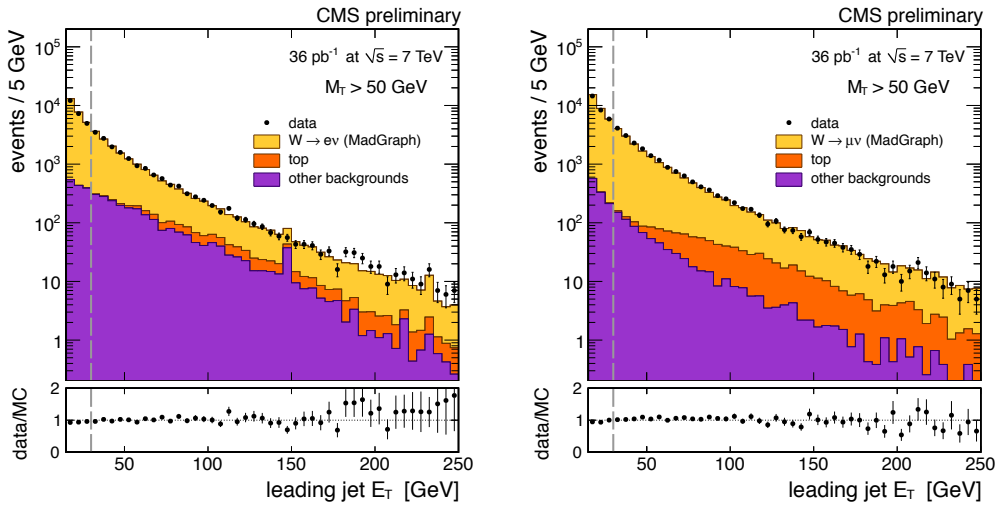


Figure 1: Distributions of the uncorrected p_T for the leading jet in the $W + 1$ jet sample for the electron channel (left) and for the muon channel (right). The ratio between the data and the simulation is also shown. The line at $p_T = 30$ GeV corresponds to the threshold imposed for counting jets.

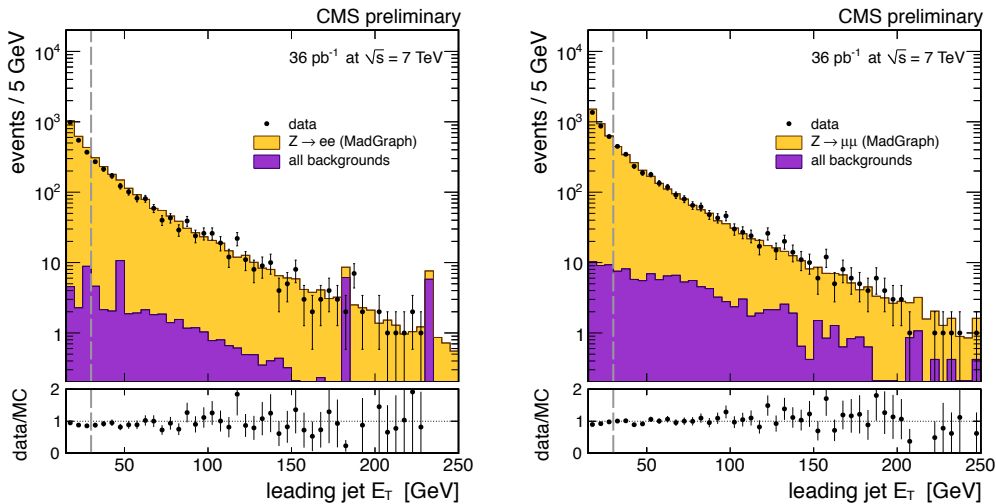


Figure 2: Distributions of the uncorrected p_T for the leading jet in the $Z + 1$ jet sample for the electron channel (left) and for the muon channel (right). The ratio between the data and the simulation is also shown. The line at $p_T = 30$ GeV corresponds to the threshold imposed for counting jets.

jet multiplicity. Since the statistical precision in the bins with $n > 1$ is insufficient, the efficiencies for these bins are extrapolated by using the p_T and η shape of the $n = 1$ bin. We find an average efficiency close to 82% for the leading p_T muon and of above 90% for the second leading muon.

6. Signal Extraction

The signal yield is extracted using an extended likelihood fit to the invariant mass, $M_{\ell+\ell-}$, for the $Z +$ jets sample and to M_T for the $W +$ jets sample. The fitting functions are parameterized on simulation and as many parameters as possible are allowed to vary in the fit.

For the Z event samples, the main background processes, dominated by $t\bar{t}$ and $W +$ jets, are small and do not produce a peak in the $M_{\ell+\ell-}$ distribution, so the $M_{\ell+\ell-}$ distribution can be split to two components, one for the signal and one for all background processes.

For the W sample, background contributions are divided into two components, one which exhibits a peaking structure in M_T , dominated by $t\bar{t}$, and another which does not, dominated by QCD multi-jet events. We perform a two-dimensional fit to the M_T distribution and the number of b -jets, $n_{b\text{-jet}}$. The M_T distribution distinguishes the signal from the non-peaking backgrounds, while $n_{b\text{-jet}}$ distinguishes the signal and the other

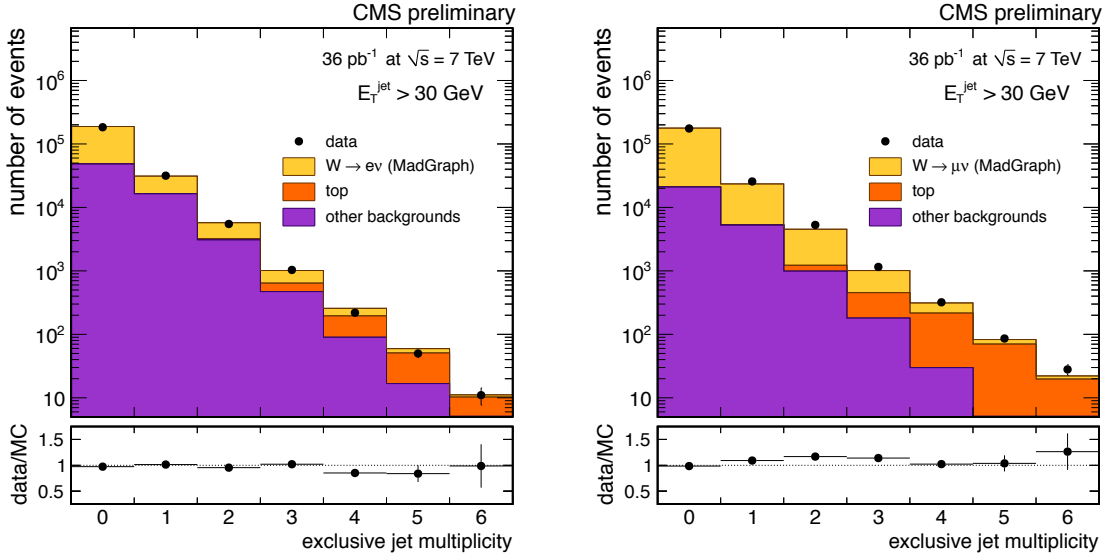


Figure 3: Exclusive number of reconstructed jets in events with $W \rightarrow e\nu$ (left) and $W \rightarrow \mu\nu$ (right). The histograms represent the expectations based on simulated events.

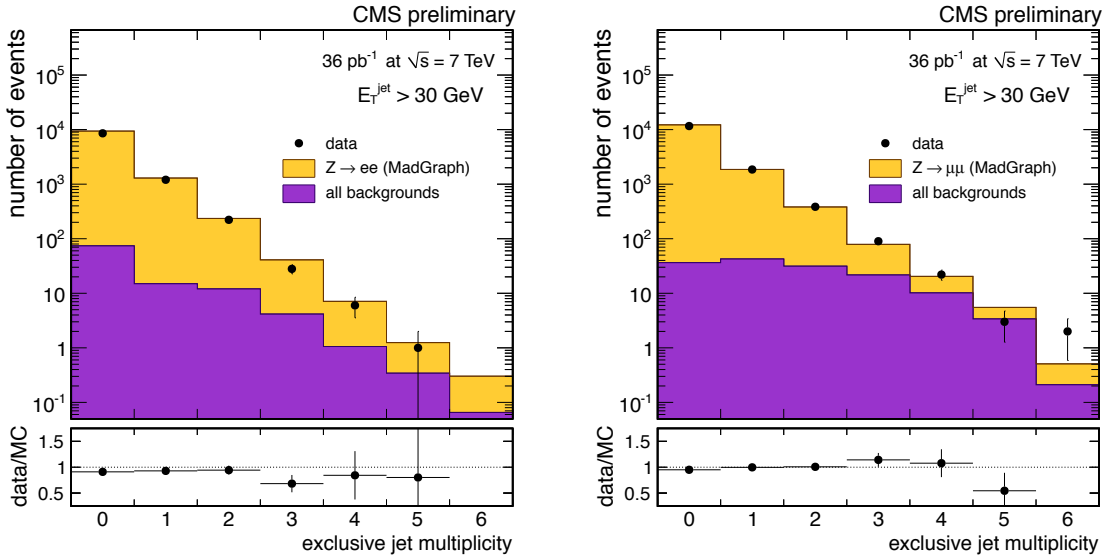


Figure 4: Exclusive number of reconstructed jets in events with $Z \rightarrow e^+e^-$ (left) and $Z \rightarrow \mu\mu$ (right). The histograms represent the expectations based on simulated events.

backgrounds from $t\bar{t}$. The likelihood fit is built on the assumption that the signal has no b-jets. This implies that a component of W produced in association with heavy flavor jets is counted as background. Considering the statistical precision of the measurement, this assumption has negligible effects on the W + jets cross section calculation.

The fits are done in exclusive jet multiplicity bins for $n \leq 3$ and inclusively for the last bin of jet multiplicity, *i.e.* $n \geq 4$. Examples of fits for $Z + 1$ jet are shown in Figure 5. Figures 6 and 7 show fits in M_T and $n_{b\text{-jet}}$ projections for $W + n$ jets ($n=1$ and $n=3$). The presence of the top background is evident comparing the $n = 1$ and $n = 3$ exclusive multiplicity bins.

In the electron channel, exclusive V + jets rates are corrected for electron efficiencies as discussed in Section 5. In the muon channel, efficiencies depend on the lepton p_T and η and on the jet multiplicity. To account for these variations, every event is assigned a weight and the fit is performed to a weighted distribution.

A second fit is performed in order to test Berends-Giele scaling and measure the associated parameters. Events are assigned to exclusive jet multiplicity bins and the yields are fit with the assumption that they conform to a

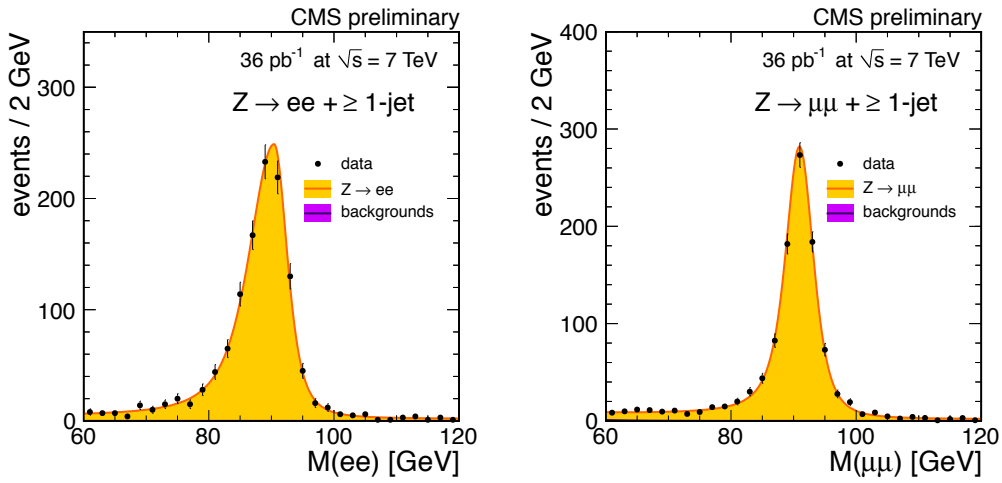


Figure 5: Di-lepton mass fit for the $Z + 1$ jet samples, in the electron channel (left) and the muon channel (right). The background is very low, rendering hardly visible in the figure.

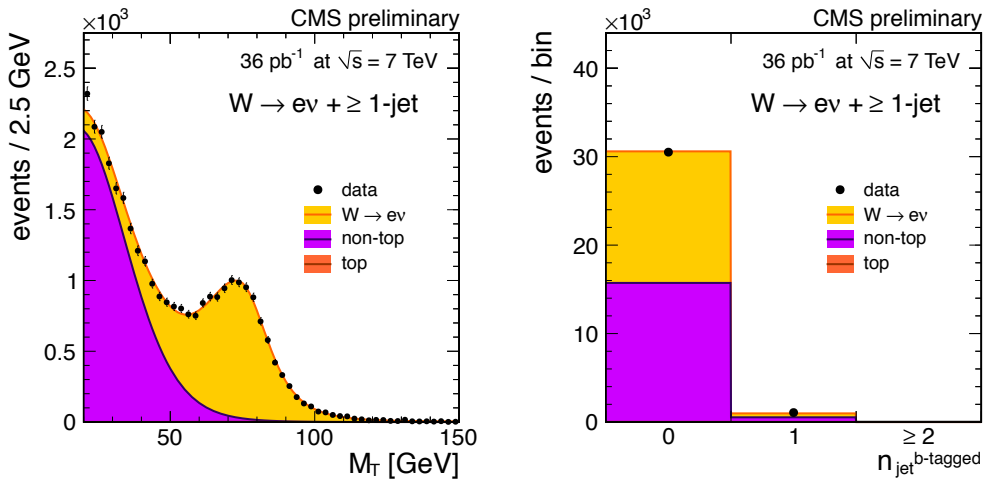


Figure 6: Fit results for the $W(e\nu) + n$ jet sample with $n = 1$. On the left is the M_T projection, and on the right $n_{b\text{-jet}}$.

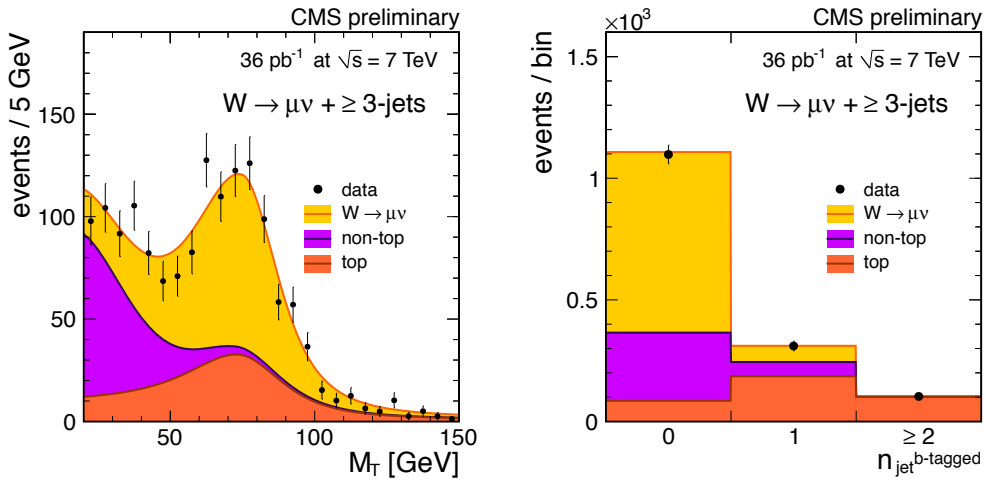


Figure 7: Fit results for the $W(\mu\nu) + n$ jet sample with $n = 3$. On the left is the M_T projection, and on the right $n_{b\text{-jet}}$.

scaling function:

$$C_n = \frac{\sigma_n}{\sigma_{n+1}} \quad (1)$$

where $\sigma_n = \sigma(V + n \text{ jets})$. To first order one expects $C_n = \alpha$, where the constant α is proportional to the inverse of the strong coupling constant, α_S^{-1} . Phase space effects can violate this simple proportionality, so we introduce a second parameter, β , to allow for a deviation from a simple constant scaling law: $C_n = \alpha + \beta n$. Due to the different kinematics of the $n = 0$ sample, the scaling expressed in Eq. (1) is not expected to hold, so we do not include the $n = 0$ sample in the fit.

7. Unfolding

In order to estimate the scaling rule of jets at the *particle level*, we apply an unfolding procedure that removes the effects of jet energy resolution and reconstruction efficiency. A migration matrix, which relates a number n' of produced jets at particle level to an observed number n of reconstructed jets, is derived from simulated samples of Z + jets and W + jets with leptons and jets within their acceptances.

We employ two well-known unfolding methods. The base line method is the ‘‘singular value decomposition’’ (SVD) method [10]. As a cross check, we apply the iterative or ‘‘Bayesian’’ method [11]. Both algorithms require a regularization parameter, chosen to be $k_{SVD} = 5$ and $k_{Bayes} = 4$, to prevent the statistical fluctuations in the data from appearing as structure in the unfolded distribution.

8. Systematic Uncertainties

One of the main sources of systematic uncertainties in the W/Z+jets measurements is the jet energy scale (JES), which affects the jet counting. The effect of jet energy uncertainties is evaluated on the jet multiplicity distribution using simulations. Compatible results have been found in all the channels, for both W and Z events. The pile-up subtraction was also tested comparing the jet multiplicity in two simulated signal samples, one without pile-up, and one with pile-up plus pile-up subtraction applied. The difference is found to be below 5%.

While the systematic uncertainty in the jet counting is correlated among the different jet multiplicities, all other uncertainties, such as from efficiency and fits, are uncorrelated between jet multiplicities. All statistical and both types of systematic uncertainties are propagated in the unfolding procedure. Finally, to estimate uncertainties in the unfolding procedure itself, we calculated the difference in unfolding using the Bayes algorithm versus the SVD algorithm, and using two different simulations, MADGRAPH and PYTHIA, for the unfolding matrix, and two different tunes, Z2 and D6T for the unfolding matrix. The resulting uncertainties are shown with the final results in the next section.

9. Results and Conclusions

From the unfolded exclusive jet multiplicity distributions we derive inclusive jet multiplicities and calculate two sets of ratios. The first set of ratios is $\sigma(V + n \text{ jets})/\sigma(V)$, where $\sigma(V)$ is the inclusive cross section, see the upper frames of Figs. 8–9. The second set of ratios is $\sigma(V + n \text{ jets})/\sigma(V + (n - 1) \text{ jets})$, shown in the lower frames of Figs. 8–9. The systematic uncertainties associated with the JES and the unfolding are shown as error bands. For a large number of jets, the PYTHIA simulation fails to describe the data, while the MADGRAPH simulation agrees well, as expected.

Finally, we show the results of the fit for α and β in our treatment of Berends-Giele scaling for both W + jets and Z + jets in Fig. 10. The results are given in the (α, β) plane and are compared to the results obtained from the MADGRAPH sample. The electron and muon expected values differ mostly because of the $\Delta R > 0.3$ cut between the jets and the leptons, which is applied only in the electron channel. The ellipses correspond to 68% C.L. considering only statistical uncertainty. The arrows show the effect on the central value from the most important sources of systematic uncertainty. The measurements agree well in the Z + jets channels, and fairly well in the W + jets channel. The β parameter is within one standard deviation from zero for the W + jets case and within 0.5 standard deviation for the Z + jets. The values for W + jets and Z + jets agree with one another, as expected in the standard model. The data is found to be in reasonable agreement with the theoretical expectations with deviations that are within one or two standard deviations depending on the channel.

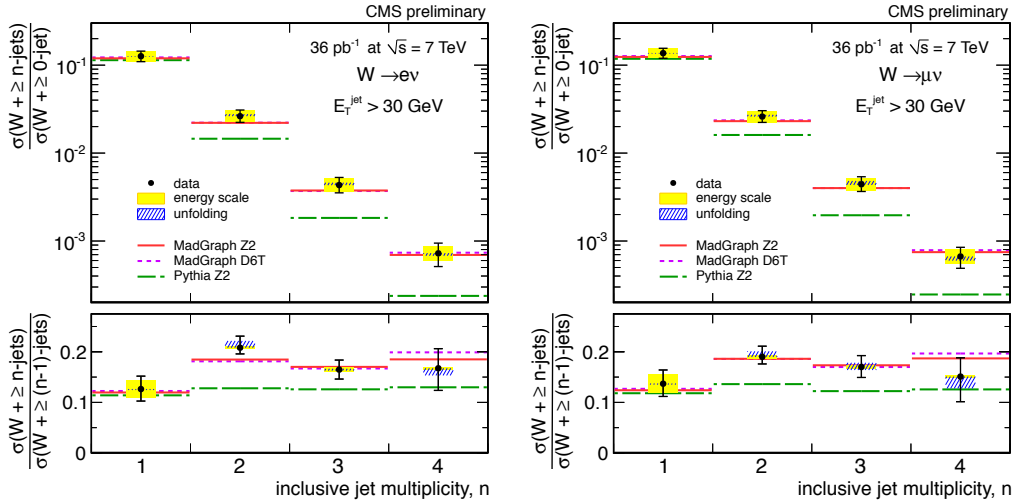


Figure 8: The ratio $\sigma(W+n \text{ jets})/\sigma(W)$ in the electron channel (left) and muon channel (right) compared to expectations from MADGRAPH and PYTHIA.

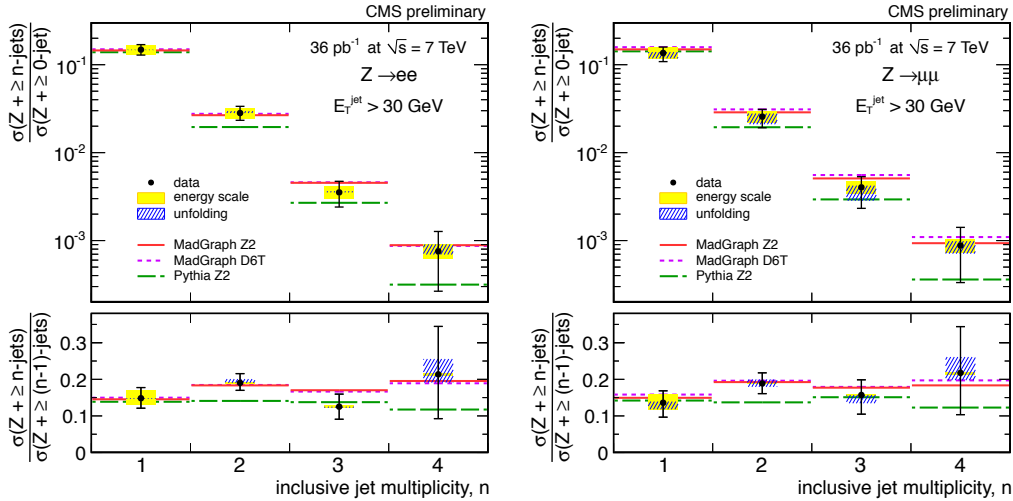


Figure 9: The ratio $\sigma(Z+n \text{ jets})/\sigma(Z)$ in the electron (left) channel and muon channel (right) compared to expectations from MADGRAPH and PYTHIA.

We measured the rate of jet production in association with a W or Z vector boson using pp collision data at $\sqrt{s} = 7$ TeV. The leading jet p_T spectrum agrees well with simulations based on MADGRAPH + PYTHIA and the Z2 tune. We unfolded the exclusive jet multiplicity distributions and measured the ratios of cross sections $\sigma(V+\geq n \text{ jets})/\sigma(V)$ and $\sigma(V+\geq n \text{ jets})/\sigma(V+\geq (n-1) \text{ jets})$ where n is the inclusive number of jets. The results are in agreement with the MADGRAPH generator. Finally, we made a quantitative test of Berends-Giele scaling. The results show good agreement between W +jets and Z +jets and fair agreement with the simulation.

Acknowledgments

I would like to acknowledge all of the people who worked extremely hard on this analysis: N. Akchurin, S.B.Beri, S. Bolognesi, A. Branca, Y. Chen, V. Ciulli, S. Dasu, B. Dahmes, J. Damgov, E. Di Marco, J. Z Efron, S. Frosali, E. Gallo, S. Gonzi, M. Grothe, P. Klabbbers, S. Lacaprara, C. Lazaridis, S. W. Lee, P. Lenzi, J.Lykken, S. Malik, M. Nespolo, P. Meridiani, M. Mozer, M. Pierini, W. Reece, C. Rogan, I. Ross, C. Rovelli, L. K. Saini, A. Schizzi, I. Segoni, A. P. Singh, M. Spiropulu, P.Traczyk, L. Vanelderen, and E. Yazgan.

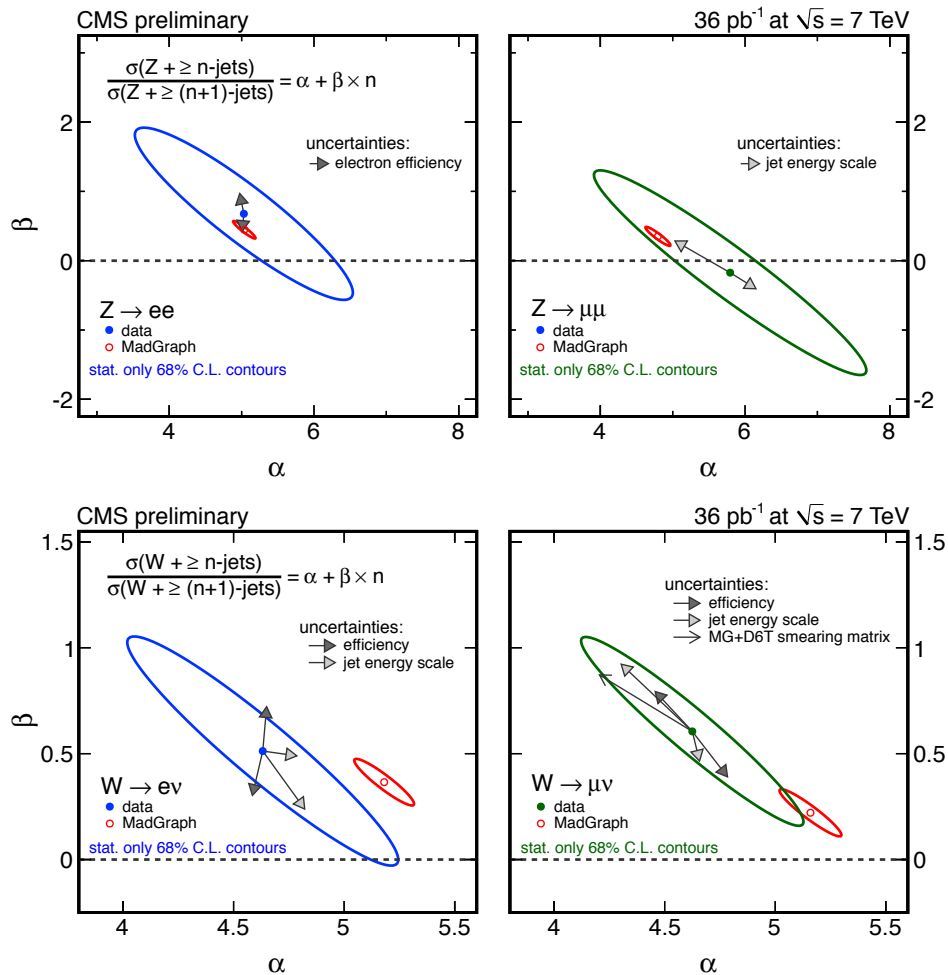


Figure 10: Fit results on the Berends-Giele scaling parameters α and β after pile-up subtraction, efficiency corrections, and unfolding for detector resolution effects. The data are compared to MADGRAPH with the Z2 tune. a) shows $Z/\gamma^* + \text{jets}$, b) shows $W + \text{jets}$.

References

- 1 Berends, Frits A. and Giele, W. T. and Kuijf, H. and Kleiss, R. and Stirling, W. James, *Multi-jet production in W, Z events at p anti-p colliders*, Phys. Lett. **B224** (1989), 237.
- 2 CMS Collaboration, *Rates of Jets Produced in Association with W and Z Bosons in pp Collisions at $\sqrt{s} = 7$ TeV*, CMS PAS **EWK-10-012** (2010).
- 3 Maltoni, Fabio and Stelzer, Tim, *MadEvent: Automatic event generation with MadGraph*, JHEP **02** (2003), 027.
- 4 Sjostrand, Torbjorn and Mrenna, Stephen and Skands, Peter Z., *PYTHIA 6.4 Physics and Manual*, JHEP **05** (2006), 026.
- 5 Field, Rick, *Early LHC Underlying Event Data - Findings and Surprises*, eprint arXiv 1010.3558 (2010).
- 6 Skands, Peter Zeiler, *Tuning Monte Carlo Generators: The Perugia Tunes*, Phys. Rev **D82** (2010), 074018.
- 7 M. Cacciari, G.P. Salam, and G. Soyez, *The anti-k_t jet clustering algorithm*, JHEP **0804** (2008), 063.
- 8 CMS Collaboration, *Measurements of Inclusive W and Z Cross Sections in pp Collisions at $\sqrt{s} = 7$ TeV*, CMS PAS **EWK-10-005** (2010).
- 9 CMS Collaboration, *Commissioning of b-jet identification with pp collisions at $\sqrt{s} = 7$ TeV*, CMS PAS **BTV-10-001** (2010).
- 10 Hocker, Andreas and Kartvelishvili, Vakhtang, *SVD Approach to Data Unfolding*, Nucl. Instrum. Meth. **A372** (1996), 469-481.
- 11 D'Agostini, G., *A Multidimensional unfolding method based on Bayes' theorem*, Nucl. Instrum. Meth. **A362** (1995), 487-498.